High quality GaN microplatelets grown by metal-organic vapor phase epitaxy on patterned silicon-on-insulator substrates: Toward micro light-emitting diodes

Kilian Baril, Pierre-Marie Coulon, Mrad Mrad, Nabil Labchir, Guy Feuillet, Matthew Charles, Cécile Gourgon, Philippe Vennéguès, Jesus Zuniga-Perez, Blandine Alloing

Journal of Applied Physics ARTICLE pubs.aip.org/aip/jap

High quality GaN microplatelets grown by metal-organic vapor phase epitaxy on patterned silicon-on-insulator substrates: Toward micro light-emitting diodes

Cite as: J. Appl. Phys. 133, 245702 (2023); doi: 10.1063/5.0149882
Submitted: 9 March 2023 · Accepted: 7 June 2023 ·
Published Online: 23 June 2023

Kilian Baril,[1,a)] Pierre-Marie Coulon,[1] Mrad Mrad,[2] Nabil Labchir,[2] Guy Feuillet,[3] Matthew Charles,[3] Cécile Gourgon,[2] Philippe Vennéguès,[1] Jesus Zuniga-Perez,[1,4] and Blandine Alloing[1]

AFFILIATIONS

[1]Université Côte d'Azur, CNRS, CRHEA, 06560 Valbonne, France
[2]LTM, Université Grenoble Alpes, CNRS, CEA/LETI-Minatec, Grenoble INP, Grenoble 38000, France
[3]Université Grenoble Alpes, CEA-LETI, 38054 Grenoble, France
[4]MajuLab, International Research Laboratory IRL 3654, CNRS, Université Côte d'Azur, Sorbonne Université, National University of Singapore, Nanyang Technological University, Singapore, Singapore

[a)]Author to whom correspondence should be addressed: kilian.baril@crhea.cnrs.fr

ABSTRACT

In this paper, we report the use of three pendeo-epitaxy growth approaches as a way of reducing the threading dislocation density (TDD) of 20 × 20 μm^2 GaN platelets to be used for the development of micro light-emitting diodes (μLEDs). The method relies on the coalescence of GaN crystallites grown on top of a network of deformable pillars etched into a silicon-on-insulator substrate. Our approach takes advantage of the creeping properties of SiO_2 at the usual GaN epitaxial growth temperature, allowing the GaN crystallites to align and reduce the grain boundary dislocations. Furthermore, this bottom-up approach allows to get rid of the dry plasma etching step for μLEDs fabrication, which highly deteriorates sidewalls, reducing the efficiency of future displays. By optimizing the growth conditions and inducing asymmetric nucleation, a TDD of 2.5 × 10^8 cm^{-2} has been achieved on the GaN platelets, while keeping a smooth surface.

INTRODUCTION

The gallium nitride (GaN) micro light-emitting diodes (μLEDs) market keeps expanding since the first report of a μLED in 2000 by Jiang *et al.*[1,2] GaN μLEDs exhibit promising properties for a wide range of applications such as displays,[3] visible light communication (VLC),[4] or biomedical devices.[5] Compared to the current organic light-emitting diode (OLED) or liquid-crystal display (LCD) technologies, μLEDs benefit from several advantages such as smaller size, longer lifetime, reduced power consumption, higher resolution, and higher brightness,[6] making them a major subject of research in academia and industry. In addition, with the market penetration of new applications such as augmented reality

(AR) and virtual reality (VR), which require even smaller pixel sizes, μLEDs technology seems to be inevitable.

However, a problem of GaN-based μLEDs, common to all other GaN-based technologies, is the lack of a physico-chemically adapted and market-compatible substrate for GaN epitaxy. While freestanding GaN substrates would be the ideal option, they remain of small dimensions and are relatively expensive. In this context, other substrates, such as sapphire and Si, have been used. In partic- ular, the heteroepitaxy of GaN on silicon (Si) has been widely studied in the last few decades to benefit from cheap and large-area substrates.[7,8] However, it displays multiple drawbacks due to the large lattice and thermal expansion coefficient mismatches as well as the melt-back etching problem arising due to the chemical

reaction between Ga and Si.[9] In addition, the difference in the lattice parameter between GaN and Si leads to high threading dislocation densities (TDDs) in GaN layers in the order of 10^{10} cm^{-2} (if nothing is done to reduce their number), which act as non-radiative centers and affects the efficiency and lifetime of the fabricated devices. The impact of the TDD on the efficiency of InGaN/GaN multiple quantum wells heterostructures was studied by Dai *et al.*[10,11] They showed that for dislocation densities varying from 5.3×10^8 to 5.7×10^9 cm^{-2}, the non-radiative coefficient A related to the Shockley–Read–Hall non-radiative recombination in the standard ABC model[12] increases from 6.10^7 to 2.10^8 s^{-1}, contributing thereby to reduce the internal quantum efficiency and validating the fact that TDD is a key parameter for improving efficiency, at least within a certain dislocation density range. Other large-area substrates based on polycrystalline AlN have been proposed as a way of growing low threading dislocation density ($\sim 10^7$ cm^{-2}) and crack-free GaN.[13] Several strategies have been employed in the past 20 years to reduce the dislocation density of GaN on Si. First, the use of interlayers, especially aluminum-based III-N interlayers, which allow the growth of thick GaN without cracks and with a dislocation density of 10^8 cm^{-2}.[14,15] Moreover, combining the use of an AlGaN interlayer, to induce a compressive strain and to prevent crack formation, and an *in situ* SiN mask, which results in bending of dislocations, low dislocation density GaN can be grown.[16,17] Although these approaches lead to a reduced TDD, they often target electronics applications where a thick GaN is acceptable. However, many optoelectronic applications need to reduce, as much as possible, the GaN thickness while keeping a low TDD. In this context, the use of a SiN interlayer coupled with an *in situ* etching method targeting dislocations has been shown to reduce the TDD down to 6.7×10^7 cm^{-2} for a total GaN thickness of 3.8 μm.[18] Second, the use of patterned substrates, which reduces the number of nucleation areas and, thus, the quantity of dislocations coming from the interface between the substrate and the GaN (or AlN) nuclei. Innovative growth techniques on patterned templates such as epitaxial layer overgrowth (ELO),[19,20] selective area overgrowth (SAG),[21,22] and pendeo-epitaxy (PE)[23–25] have led to a drastic decrease in the TDD (5×10^7 cm^{-2} in the laterally overgrown region, and 8×10^8 cm^{-2} in the opening of the mask in the case of ELOG[26]). However, the threading dislocation distribution is inhomogeneous, leading to dislocation-free zones next to high dislocation density regions (above 10^9 cm^{-2}), which correspond to the coalescence zones between neighboring GaN sections. The high TDD at the coalescence boundaries can be traced back to the misalignment of the initial AlN or GaN islands, leading to a misalignment between the overgrown regions of GaN.[27] This misalignment between nucleation grains is also responsible for the high TDD in the seed regions,[28,29] impacting the efficiency of the future overgrown devices.

Therefore, since it is known that TDD decreases the efficiency of LEDs, different strategies are implemented to reduce it. Besides, another issue specific to μLED devices has a significant impact on their efficiency, namely, the use of etching of the devices. Indeed, μdisplay technology requires a pixel size (directly related to the diameter of μLEDs) below 10 μm^2 to achieve a high spatial resolution. However, several studies have shown that the size reduction of μLEDs reduces their external quantum efficiencies (EQEs).[30–33] This phenomenon has been attributed to the standard dry plasma etching step defining μLEDs on wafers, which creates sidewall defects that are non-radiative recombination centers. This issue is a limiting factor to the growth approaches mentioned earlier on a full wafer, where the etching step is unavoidable. In this context, it would be extremely interesting to manufacture μLEDs without the use of a top-down etching step of the active LED and, thus, avoid the aforementioned sidewall damage.

In order to tackle the μ-LED issues described above, we introduce an approach that combines pendeo-epitaxy and silicon-on-insulator (SOI) substrates that are patterned into nano- pillars, on top of which GaN nucleates and grows laterally. First, to limit the creation of dislocations during the coalescence of GaN crystallites nucleating on top of the nano-pillars, an SOI substrate is used; this allows to benefit from the visco-elastic properties of SiO_2 at the high temperature employed for GaN growth.[34] The SiO_2 layer below the Si surface should allow crystallites to rotate around themselves during coalescence and minimize dislocation generation. Second, the bottom-up growth approach allows to get rid of the etching step and, therefore, of the defects associated with it. Moreover, once the substrate is patterned, the epitaxial regrowth will only be pure GaN, without resorting to interlayers based on other materials. Finally, the brittleness of the pillars is used to facilitate the transfer of full and homogeneous GaN platelets onto a carrier substrate, which can, for instance, contain the electronics necessary for controlling individually each μLED. Several transfer methods can be used and are currently being optimized.

Our earlier work[35] using a similar approach reported a reduced TDD of 4×10^8 cm^{-2} and an overall strain reduction on 300×300 μm^2 platelets. In that report two sources of dislocations were clearly identified, as we could distinguish dislocations coming from the seed regions and dislocations created during island coalescence. This study aims to further reduce the dislocation density on smaller platelets compatible with μLED requirements. It also aims to understand the growth mechanisms during nucleation of dislocations.

EXPERIMENTAL DETAILS

Silicon-on-insulator (SOI) substrates were fabricated at CEA-LETI with a 500 nm thick buried oxide (BOX) and a 50 nm thick Si 111 layer. On these substrates, an AlN buffer layer and a thin GaN layer were then grown using a Metal Organic Vapor Phase Epitaxy (MOVPE) (3×2 in.) CCS Thomas Swann reactor, with thicknesses of 125 and 250 nm, respectively. The AlN buffer layer is essential to avoid any melt-back etching reaction between Ga and Si.[9] Atomic force microscopy images performed on the GaN layer indicate a TDD in the order of 10^{10} cm^{-2}.

The samples were then patterned using nanoimprint lithography coupled with a lift-off step, as detailed in a previous publication.[36] GaN/AlN/Si/SiO_2 nano-pillars 150 nm in diameter were etched into a hexagonal pattern with a pitch of 500 nm.

These matrices of pillars form the base for the future GaN micro-platelets 20×20 μm^2 in size. The final distance between different platelets is around 10 μm—the objective is to prevent any coalescence between neighboring platelets, once the GaN growth has been achieved while keeping them close enough to avoid any parasitic growth between them.

TABLE I. Summary of the growth conditions for samples A, B, and C. The temperatures are the setpoint temperatures.

	3D growth step				
	Time (s)	Temperature (°C)	Pressure (Torr)	Carrier gas	NH3 (SCCM)/TMGa (SCCM)
Sample A (Ref) and B	100	1060	100	N_2	3000/30
Sample C	40	1060	100	N_2	3000/30
	2D growth step				
	Time (s)	Temperature (°C)	Pressure (Torr)	Carrier gas	NH_3 (SCCM)/TMGa (SCCM)
Sample A (Ref) and B	5400	1170	300	H_2	9000/80
Sample C	7200	1170	300	H_2	6000/54

The regrowth on the patterned substrates has been done using the same Thomas Swann reactor as for the buffer layers. Cathodoluminescence (CL) spectroscopy and atomic force microscopy (AFM) were used to characterize the threading dislocation density of the samples.[37] In addition, scanning electron microscopy (SEM) and transmission electron microscopy (TEM) give an insight into the growth mechanisms and how they affect dislocation filtering.

Three samples (A, B, and C) were grown using conditions given in Table I, with trimethylgallium (TMGa) and ammonia (NH_3) as precursors. The growth temperatures given in Table I and in the rest of this study are the setpoint temperatures.

In order to lower the dislocation density, a two-step growth has been used (Fig. 1), similar to our previous study.[35] Nucleation on top of nano-pillars occurs during the first step, where conditions were optimized for a pyramidal 3D growth of GaN.[38] The V/III ratio was fixed to 1850 for all samples (A, B, and C). The three samples differ either in the structure of the pillars (samples A and B, without and with SiO_2 mask on top, respectively), which modify the nucleation, or in the coalescence mode employed (samples A and C using homogenous and inhomogeneous nucleation, respectively). Upon the formation of GaN pyramids, a higher temperature 2D growth step was used to coalesce the individual pyramids and planarize the GaN platelets.

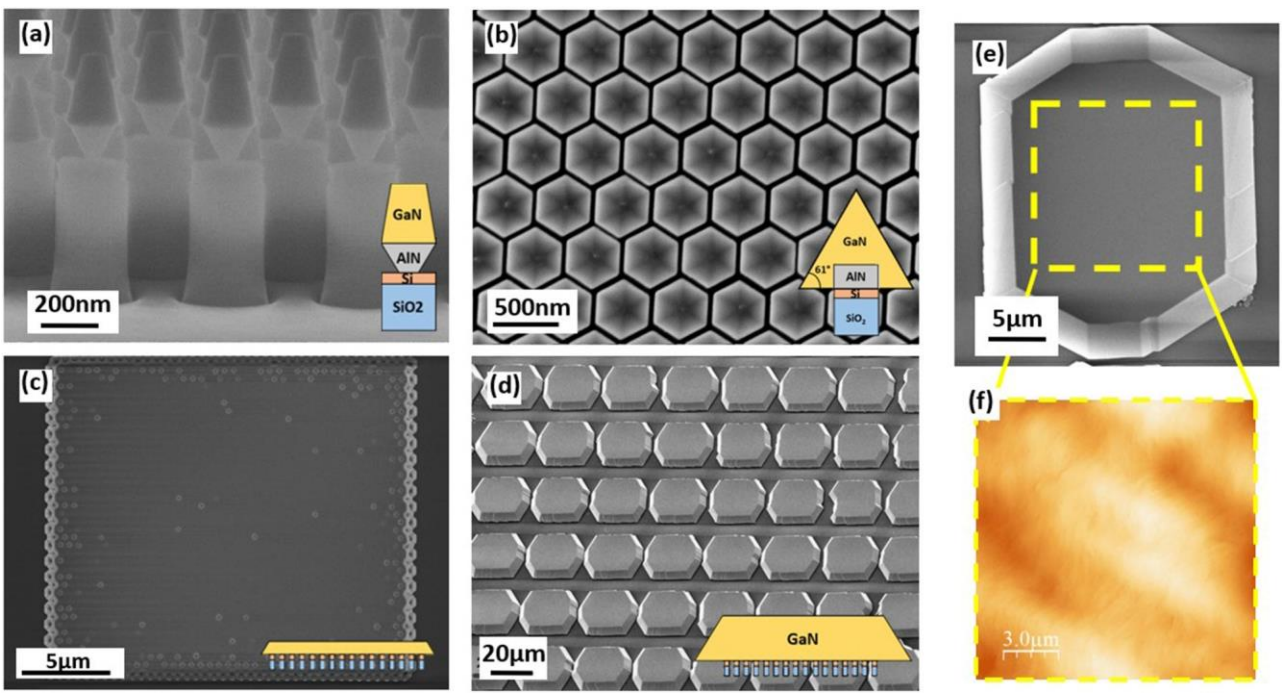

FIG. 1. SEM images: cross section of the patterned sample before regrowth (a), after 3D GaN growth in top view (b), after 30 min of 2D growth in top view (c), and after 90 min of 2D growth to obtain fully coalesced platelet with a tilted view of 30° (d). A schematic is provided as in the inset of each SEM image for clarity. Magnified SEM view of a single platelet (e) with the corresponding $15 \times 15\ \mu m^2$ AFM scan of the surface (f).

RESULTS AND DISCUSSION

In order to facilitate the reading of this study, we recall here the definitions and sizes of the different objects which are the subject of this study: (i) the 150 nm diameter pillars etched in the substrate, which can be seen in Figs. 1(a), 3(a), and 5(a); (ii) the GaN pyramids at the top of the pillars [Figs. 1(b), 3(b), and 5(b)], with a maximum base diameter of 250 nm; (iii) the individual 20 × 20 μm^2 platelets consisting of a set of coalesced pyramids [Figs. 1(c), 3(c), and 5(c)]; (iv) the 500 × 500 μm^2 platelet arrays, which can be partially seen in Figs. 1(d), 3(d), 5(d) and seen completely in Fig. 6(d).

SAMPLE A: REFERENCE SAMPLE

Figure 1 presents the regrowth steps (both 3D and 2D growth steps) of our reference sample A, with similar growth conditions to our previous study.[35] Figure 1(a) shows a SEM cross section view of the GaN/AlN/Si/SiO_2 pillars after plasma etching and a CARO treatment (H_2O_2 + H_2SO_4), which was employed to remove the nickel mask on top of the pillars. An under etching of the AlN layer is observed during this treatment, leading to a reduced pillar diameter at the interface between AlN and Si. The first regrowth step is shown in Fig. 1(b), with a top view SEM image of the 3D GaN pyramids on top of the pillars. GaN pyramids show six semipolar {10-11} facets due to the anisotropic growth rate of GaN. Then, Fig. 1(c) shows a top view SEM image of a platelet after a 30 min growth in the 2D growth step conditions. The sample exhibits an almost complete coalescence between pyramids with a recovery of the c-plane for a GaN thickness of less than 2 μm. However, some V-shaped pits are still present on the surface. Finally, Fig. 1(d) shows a tilted view of fully coalesced 5 μm thick GaN platelets for a growth time of 90 min in the 2D growth step conditions. The final grown platelets present a reduced *c*-plane surface compared to the initial pattern and pillar positions. This is due to the growth of more stable semipolar facets along the perimeter of each platelet. Those facets have been recently shown to be beneficial for the light extraction of μLEDs.[39,40] Figures 1(e) and 1(f) show a magnified view of a single platelet surface using SEM and AFM, respectively. The width of the AFM scan is limited to 15 μm to avoid any sliding into the semipolar facets. The surface is smooth with a RMS of 2 nm and does not exhibit any v-pits.

The TDD has been investigated by combining multiple 2× 2 μm^2 AFM images [Fig. 2(a)] on several platelets and by using large-area CL images [Fig. 2(c)]. This methodology gives a statistically meaningful average TDD value.[37] Both AFM and CL give similar results, with an average TDD of 4 ± 1 × 10^8 cm^{-2}, comparable to our previous work on larger-size GaN platelets.[35]

SAMPLE B: MASKED PENDEO-EPITAXY

Sample B presents an alternative approach for managing dislocations coming from the nitrides/Si initial growth and makes use of a 30 nm thick SiO_2 mask on top of each GaN/AlN/Si/SiO_2 pillar. This additional SiO_2 layer is deposited on the GaN/AlN/SOI 2D stack by physical vapor deposition before nanoimprint lithography. As in conventional ELOG, SiO_2 will act as a dielectric mask blocking dislocations.[41] Figure 3(a) shows a cross section SEM image of

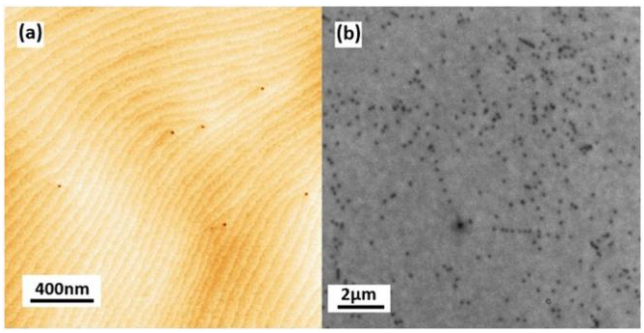

FIG. 2. 2× 2 μm^2 AFM (a) and 14 × 14 μm^2 CL (b) images of a GaN platelet surface (i.e., after the 2D growth step) of sample A.

sample B before regrowth. The SiO_2 layer can be seen on top of each pillar in a brighter contrast. Figure 3(b) shows the 3D growth step on sample B. GaN pyramids have a pit at the apex, due to the growth over the SiO_2 mask. The growth conditions are exactly the same as for the reference sample. Figure 3(c) shows an SEM image after 30 min of lateral growth. The surface is comparable to sample A in the same conditions [Fig. 1(c)] with several v-pits on the surface. However, the SiO_2 mask on top of the pillars does not seem to create additional v-pits. Finally, Fig. 3(d) shows fully coalesced platelets with the same growth conditions as sample A [Fig. 1(d)]. As for sample A, no v-pits are visible on the surface of the platelets.

Scanning transmission electron microscopy (STEM) observations were performed on both reference sample A and sample B in

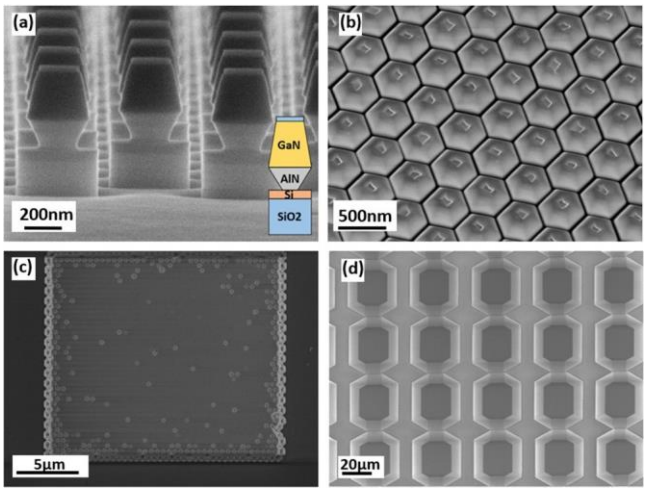

FIG. 3. SEM images of sample B at different fabrication steps: cross section of nano-pillars with a 30 nm-thick SiO_2 mask before growth (a), a tilted view of 30° after the 3D GaN growth (b), top view after a 30 min 2D growth step (c), and after a complete 2D growth step of 90 min (d).

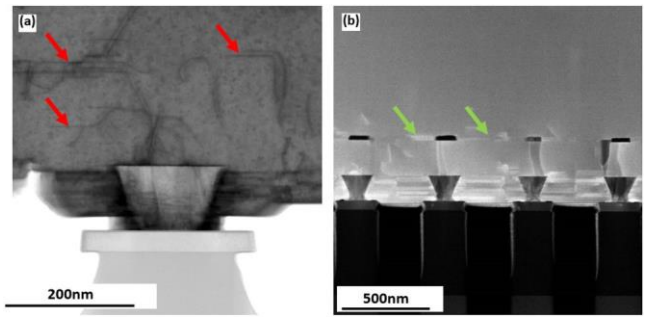

FIG. 4. Scanning transmission electron microscopy of the regrown GaN layer on top of nano-pillars of sample A (a) and sample B with a SiO_2 mask (b) with the yellow dashed lines showing the initial GaN pyramid, red arrows showing the bent dislocations, and green arrows showing the dislocation created at the vicinity of the GaN/SiO_2 interface.

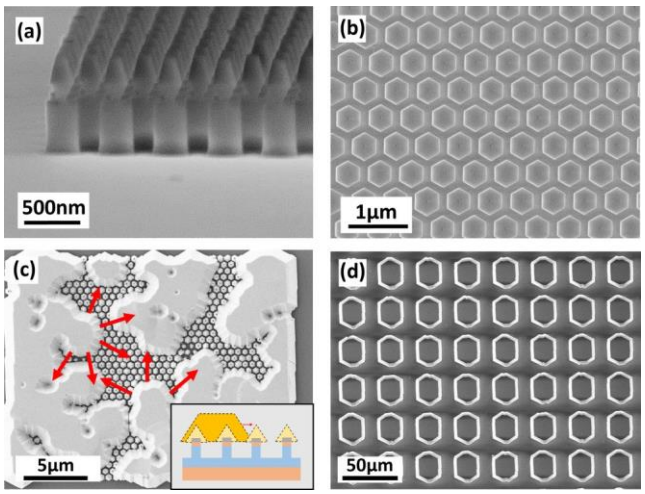

FIG. 5. Cross section view by SEM of pillars before any regrowth (a), top view of the GaN pyramids at the end of the 3D growth (b), top view SEM images of the asymmetric cluster nucleation on GaN pyramids with the scheme in inset (c), and the platelets array after being fully coalesced (d).

order to compare the behavior of dislocations. A thin lamella has been prepared using a focus ion beam (FIB) tool with the (11-20) zone axis passing through the pillars. Figure 4 shows STEM images of the two samples. First, in Fig. 4(a), we observe that the regrown GaN nucleates both on the GaN layer and also on the underlying AlN. A large number of dislocations is generated at the regrown-GaN/initial-AlN sidewalls. Those dislocations are initially confined to the basal plane, but can potentially bend toward the top surface (as well as toward the bottom free surface) during island coalescence, leading to an increased TDD.

Figure 4(a) also shows the typical dislocation bending observed previously in 3D GaN pyramids (red arrows), in which dislocations bend into the basal planes when they meet a semipolar facet. The pyramidal shape before the lateral growth is indicated by the dashed yellow lines, which defines clearly the boundary at which dislocation bending occurs. This mechanism, reported first by Vennéguès *et al.*,[41] and subsequently in several other papers,[42] has been commonly adopted for TDD reduction in both GaN-on-Si and GaN-on-Sapphire systems. These bent dislocations propagate laterally and, thus, have a certain probability of creating dislocation loops during coalescence, which would reduce the TDD. However, they might also bend again and thread toward the surface, resulting in no net reduction in TDD.

Figure 4(b) shows different behavior, with vertical dislocations originating from the AlN/Si nucleation interface being blocked by the SiO_2 mask. However, new dislocations are generated in the vicinity of the GaN/SiO_2 (mask) interface, as observed in some SAG of GaN nano/microwires on patterned substrates.[43]

The TDD of sample B has been quantified using the same methodology as sample A on several platelets. Again, both AFM and CL give similar results, with the same average TDD of $4\pm 1\times 10^{8}$ cm^{-2} as sample A. The equivalence between samples A and B in terms of the final TDD can be explained by the fact that both approaches target the same problem, namely, the dislocations nucleating at the pillars.

In consequence, we can suggest that most of the remaining threading dislocations are coming from the pyramid coalescence. This means that there are still misorientations remaining between neighboring islands. This possible reorientation of GaN crystallites during coalescence has been studied on similar samples in a recent work using dark field x-ray microscopy and high-intensity x-ray diffraction at the European Synchrotron Radiation Facility. We have shown that local realignment of GaN crystallites occurred during coalescence, while the Si layer underneath GaN was being disoriented during coalescence showing that, indeed, the SiO_2 section contributed to the pillar's rotations.[44]

In both approaches for samples A and B, reducing the density of nucleation sites should decrease the number of coalescence grain boundaries and, thereby, the TDD. The obvious solution would consist in increasing the distance between pillars, but this would increase the parasitic growth nucleation on the mask.

SAMPLE C: INHOMOGENEOUS REGROWTH SITES

In order to get around this problem and still reduce the number of coalescence grain boundaries without sacrificing the GaN thickness, we introduce an original approach based on the generation of controlled but inhomogeneously distributed regrowth sites during the coalescence step (i.e., during the 2D growth step). We start from the same pillars as sample A, shown in Fig. 5(a). Then the pyramids are grown, but with a shorter 3D growth step, leaving the pyramids further apart from one another [Fig. 5(b)]. The precursor flows during the coalescence step are reduced compared to the conditions used for samples A and B (we maintain the same V/III ratio, but reduce the flows by 30%), and GaN clusters then nucleate on top of the pyramid network. This is illustrated in Fig. 5(c), for 30 min of lateral growth. This should be compared to a completely homogenous lateral growth observed in samples A and B [Figs. 1(c) and 3(c)].

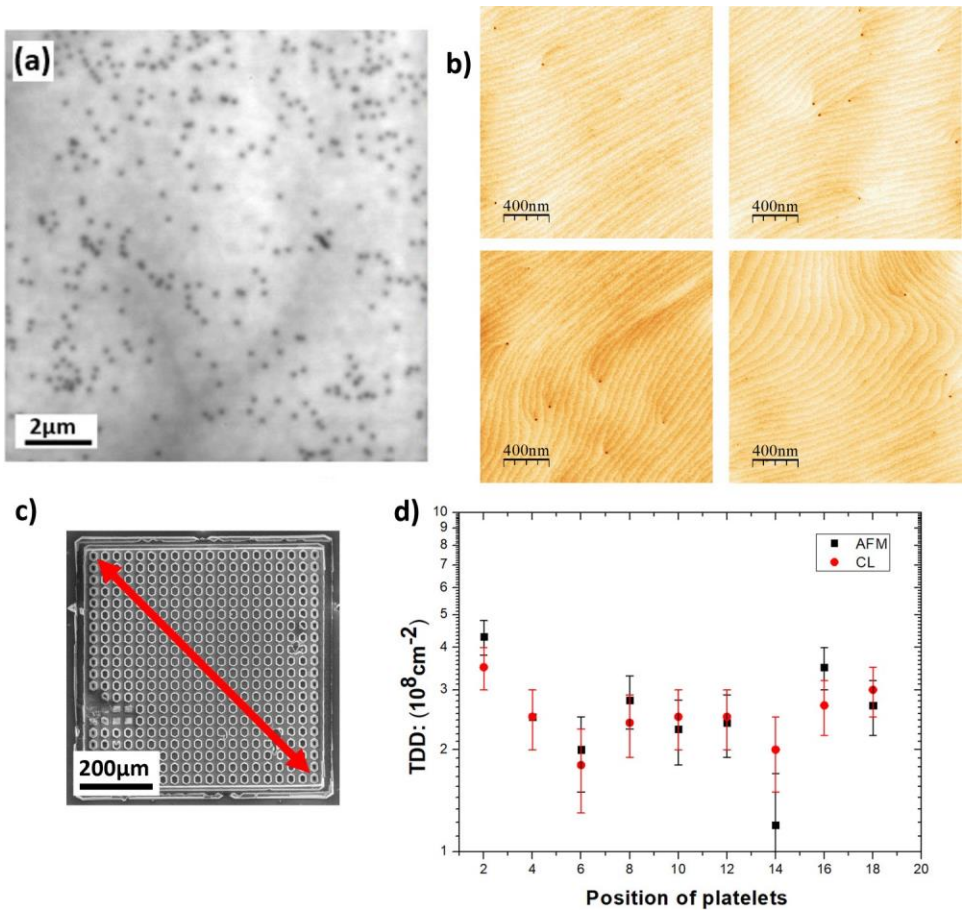

FIG. 6. CL (a) and AFM (b) images on fully coalesced platelets after asymmetric cluster nucleation; (c) a platelets array; and (d) the TDD measurements along the diagonal of the array.

The cluster nucleation, in particular, its density,[45] is controlled by the growth conditions. We have found that the inhomogeneity of nucleation is mainly determined by the precursor fluxes and by the distance between GaN pyramids at the end of the first 3D growth step. In order to promote the formation of such clusters, the 3D growth step leading to pyramid formation must be stopped before pyramids begin to coalesce. If pyramids come into contact, the lateral growth will then be homogeneous.

As for samples A and B, smooth 5 μm-thick GaN platelets are obtained by continuing the growth [Fig. 5(d)].

Figure 6 shows the threading dislocation density on sample C using both AFM and CL on the platelets along the diagonal of an array of platelets (array defined by the presence of a continuous square trench, visible in Fig. 6(c)]. The average TDD for sample C is found to be 2.5 ± 1.10^8 cm^{-2}, this TDD being a factor nearly ~2 lower than that of samples A and B. Figures 6(c) and 6(d) show that the TDD remains relatively constant across the diagonal of the platelet array, demonstrating that results are reproducible. This decrease in the TDD is explained by the reduction in the number of grain boundaries. Coalescence does not occur between each pyramid but between a smaller number of clusters covering the pyramids.

CONCLUSION

In this study, the growth of arrays of 20 × 20 μm^2 GaN platelets has been investigated with the aim of reducing the threading dislocation density, while keeping the total thickness as low as possible. The use of a patterned SOI substrate allows a bottom-up growth approach that avoids the dry plasma etching step that deteriorates μLED sidewalls, leading to a reduction of their external quantum efficiency. Two innovative approaches relying on pendeo-epitaxy (namely, masked pendeo-epitaxy and inhomogeneous clustering) were investi- gated in order to achieve an excellent low threading dislocation density of 2.5×10^8 cm^{-2}.

ACKNOWLEDGMENTS

The authors would like to thank the French National Nanofabrication Network (RENATECH) and the Upstream Technological Platform (PTA) for their assistance and technical support. This work was supported by the French ANR via CARNOT and ANR-20-CE24-0022.

AUTHOR DECLARATIONS

Conflict of Interest

The authors have no conflicts to disclose.

Author Contributions

Kilian Baril: Writing – original draft (equal). Pierre-Marie Coulon: Writing – review & editing (equal). Mrad Mrad: Resources (equal). Nabil Labchir: Writing – review & editing (equal). Guy Feuillet: Conceptualization (equal). Matthew Charles: Supervision (equal); Writing – review & editing (equal). Cécile Gourgon: Writing – review & editing (equal). Philippe Vennéguès: Writing – review & editing (equal). Jesus Zuniga-Perez: Supervision (equal); Writing – review & editing (equal). Blandine Alloing: Supervision (equal); Writing – review & editing (equal).

DATA AVAILABILITY

The data that support the findings of this study are available within the article.

REFERENCES

[1]H. X. Jiang, S. X. Jin, J. Li, J. Shakya, and J. Y. Lin, "III-nitride blue microdisplays," Appl. Phys. Lett. 78(9), 1303 (2001).

[2]S. X. Jin, J. Li, J. Z. Li, J. Y. Lin, and H. X. Jiang, "GaN microdisk light emitting diodes," Appl. Phys. Lett. 76(5), 631–633 (2000).

[3]F. Templier, "GaN-based emissive microdisplays: A very promising technology for compact, ultra-high brightness display systems," J. Soc. Inf. Disp. 24(11), 669–675 (2016).

[4]R. X. G. Ferreira, E. Xie, J. J. D. Mckendry, S. Rajbhandari, H. Chun, G. Faulkner, S. Watson, A. E. Kelly, E. Gu, R. V. Penty, I. H. White, D. C. O'brien, and M. D. Dawson, "High bandwidth GaN-based micro-LEDs for multi-Gb/s visible light communications," IEEE Photonics Technol. Lett. 28(19), 2023–2026 (2016).

[5]H. E. Lee, J. H. Shin, J. H. Park, S. K. Hong, S. H. Park, S. H. Lee, J. H. Lee, I. S. Kang, and K. J. Lee, "Micro light-emitting diodes for display and flexible biomedical applications," Adv. Funct. Mater. 29(24), 1808075 (2019).

[6]J. Y. Lin and H. X. Jiang, "Development of microLED," Appl. Phys. Lett. 116(10), 100502 (2020).

[7]F. Semond, "Epitaxial challenges of GaN on silicon," MRS Bull. 40(5), 412–417 (2015).

[8]I. C. Kizilyalli, P. Bui-Quang, D. Disney, H. Bhatia, and O. Aktas, "Reliability studies of vertical GaN devices based on bulk GaN substrates," Microelectron. Reliab. 55(9–10), 1654–1661 (2015).

[9]M. Khoury, O. Tottereau, G. Feuillet, P. Vennéguès, and J. Zúñiga-Pérez, "Evolution and prevention of meltback etching: Case study of semipolar GaN growth on patterned silicon substrates," J. Appl. Phys. 122(10), 105108 (2017).

[10]Q. Dai, M. F. Schubert, M. H. Kim, J. K. Kim, E. F. Schubert, D. D. Koleske, M. H. Crawford, S. R. Lee, A. J. Fischer, G. Thaler, and M. A. Banas, "Internal quantum efficiency and nonradiative recombination coefficient of GaInN/GaN multiple quantum wells with different dislocation densities," Appl. Phys. Lett. 94, 111109 (2009).

[11]A. Armstrong, T. A. Henry, D. D. Koleske, M. H. Crawford, K. R. Westlake, and S. R. Lee, "Dependence of radiative efficiency and deep level defect incorporation on threading dislocation density for InGaN/GaN light emitting diodes," Appl. Phys. Lett. 101(16), 162102 (2012).

[12]S. Karpov, "ABC-model for interpretation of internal quantum efficiency and its droop in III-nitride LEDs: A review," Opt. Quantum Electron. 47(6), 1293–1303 (2015).

[13]A. Tanaka, W. Choi, R. Chen, R. Liu, W. M. Mook, K. L. Jungjohann, P. K. L. Yu, and S. A. Dayeh, "Structural and electrical characterization of thick GaN layers on Si, GaN, and engineered substrates," J. Appl. Phys. 125(8), 082517 (2019).

[14]E. Feltin, B. Beaumont, M. Laügt, P. de Mierry, P. Vennéguès, H. Lahrèche, M. Leroux, and P. Gibart, "Stress control in GaN grown on silicon (111) by metalorganic vapor phase epitaxy," Appl. Phys. Lett. 79(20), 3230–3232 (2001).

[15]A. Dadgar, J. Bläsing, A. Diez, A. Alam, M. Heuken, and A. Krost, "Metalorganic chemical vapor phase epitaxy of crack-free GaN on Si(111) exceeding 1 μm in thickness," Jpn. J. Appl. Phys. 39(11B), L1183–12 (2000).

[16]T. Hikosaka, H. Yoshida, N. Sugiyama, and S. Nunoue, "Reduction of threading dislocation by recoating GaN island surface with SiN for high-efficiency GaN-on-Si-based LED," physica status solidi c 11(3–4), 617–620 (2014).

[17]K. Cheng, M. Leys, S. Degroote, M. Germain, and G. Borghs, "High quality GaN grown on silicon(111) using a Six Ny interlayer by metal-organic vapor phase epitaxy," Appl. Phys. Lett. 92(19), 192111 (2008).

[18]K. Matsumoto, T. Ono, Y. Honda, T. Yamamoto, S. Usami, M. Kushimoto, S. Murakami, and H. Amano, "Reduction of dislocations in GaN on silicon substrate using *In situ* etching," Phys. Status Solidi B 255(5), 1700387 (2018).

[19]O. Nam, T. S. Zheleva, M. D. Bremser, and R. F. Davis, "233 lateral epitaxial overgrowth of GaN films on SiO 2 areas via MOVPE," J. Electron. Mater. 27(4), 233–237 (1998).

[20]S. Dassonneville, A. Amokrane, B. Sieber, J. L. Farvacque, B. Beaumont, and P. Gibart, "Luminescence of epitaxial GaN laterally overgrown on (0001) sapphire substrate: Spectroscopic characterization and dislocation contrasts," J. Appl. Phys. 89(7), 3736–3743 (2001).

[21]S. Tanaka, Y. Kawaguchi, N. Sawaki, M. Hibino, and K. Hiramatsu, "Defect structure in selective area growth GaN pyramid on (111)Si substrate," Appl. Phys. Lett. 76(19), 2701–2703 (2000).

[22]A. Tanaka, W. Choi, R. Chen, and S. A. Dayeh, "Si complies with GaN to overcome thermal mismatches for the heteroepitaxy of thick GaN on Si," Adv. Mater. 29(38), 1702557–1702556 (2017).

[23]T. S. Zheleva, S. A. Smith, D. B. Thomson, K. J. Linthicum, P. Rajagopal, and R. F. Davis, "Pendeo-epitaxy: A new approach for lateral growth of gallium nitride films," J. Electron. Mater. 28(4), L5 (1999).

[24]U. T. Schwarz, P. J. Schuck, M. D. Mason, R. D. Grober, A. M. Roskowski, S. Einfeldt, and R. F. Davis, "Microscopic mapping of strain relaxation in uncoalesced pendeoepitaxial GaN on SiC," Phys. Rev. B 67(4), 1–4 (2003).

[25]P. Shields, C. Liu, A. Šatka, A. Trampert, J. Zúñiga-Pérez, B. Alloing, D. Haško, F. Uherek, W. Wang, F. Causa, and D. Allsopp, "Nanopendeo coalescence overgrowth of GaN on etched nanorod array," Phys. Status Solidi C 8(7–8), 2334–2336 (2011).

[26]E. Feltin, B. Beaumont, P. Vennéguès, T. Riemann, J. Christen, J. P. Faurie, and P. Gibart, "Epitaxial lateral overgrowth of GaN on silicon (111)," Phys. Status Solidi A 188, 733–737 (2001).

[27]N. Mante, S. Rennesson, E. Frayssinet, L. Largeau, F. Semond, J. L. Rouvière, G. Feuillet, and P. Vennéguès, "Proposition of a model elucidating the AlN-on-Si (111) microstructure," J. Appl. Phys. 123(21), 215701 (2018).

[28]S. I. Nagahama, N. Iwasa, M. Senoh, T. Matsushita, Y. Sugimoto, H. Kiyoku, T. Kozaki, M. Sano, H. Matsumura, H. Umemoto, K. Chocho, and T. Mukai, "High-power and long-lifetime InGaN multi-quantum-well laser diodes grown on low-dislocation-density GaN substrates," Jpn. J. Appl. Phys. 39(7A), L647 (2000).

[29]Z. Liliental-Weber and D. Cherns, "Microstructure of laterally overgrown GaN layers," J. Appl. Phys. 89(12), 7833 (2001).

[30]P. Tian, J. J. D. Mckendry, and Z. Gong, "Size-dependent efficiency and efficiency droop of blue InGaN micro-light emitting diodes," Appl. Phys. Lett. 101, 231110 (2012).

[31]F. Olivier, S. Tirano, L. Dupré, B. Aventurier, C. Largeron, and F. Templier, "Influence of size-reduction on the performances of GaN-based micro-LEDs for display application," J. Lumin. 191, 112–116 (2017).

[32]R. H. Horng, C. X. Ye, P. W. Chen, D. Iida, K. Ohkawa, Y. R. Wu, and D. S. Wuu, "Study on the effect of size on InGaN red micro-LEDs," Sci. Rep. 12(1), 1324 (2022).
[33]J. M. Smith, R. Ley, and M. S. Wong, "Comparison of size-dependant characteristics of blue and green InGaN microLEDsdown to 1 μm in diameter," Appl. Phys. Lett. 116, 071102 (2020).
[34]J. Cao, D. Pavlidis, and Y. Park, "Improved quality GaN by growth on compliant silicon-on-insulator substrates using metalorganic chemical vapor deposition," J. Appl. Phys. 83, 3829 (1998).
[35]R. Dagher, P. de Mierry, B. Alloing, V. Brändli, M. Portail, B. Damilano, N. Mante, N. Bernier, P. Gergaud, M. Cottat, C. Gourgon, J. Z. Perez, and G. Feuillet, "Pendeo-epitaxy of GaN on SOI nano-pillars: Freestanding and relaxed GaN platelets on silicon with a reduced dislocation density," J. Cryst. Growth 526, 125235 (2019).
[36]M. Mrad, K. Baril, M. Charles, J. Z. Perez, S. Labau, M. Panabiere, C. Petit-Etienne, B. Alloing, G. Lefevre, L. Dupré, G. Feuillet, and C. Gourgon, "Controlled SOI nanopatterning for GaN pendeo-epitaxy," Micro Nano Eng. 14, 100110 (2022).
[37]M. Khoury, A. Courville, B. Poulet, M. Teisseire, E. Beraudo, M. J. Rashid, E. Frayssinet, B. Damilano, F. Semond, O. Tottereau, and P. Vennéguès, "Imaging and counting threading dislocations in c-oriented epitaxial GaN layers," Semicond. Sci. Technol. 28(3), 035006 (2013).
[38]P. Gibart, B. Beaumont, and P. Vennéguès, "Epitaxial lateral overgrowth of GaN," in *Nitride Semiconductors: Handbook on Materials and Devices* (Wiley - VCH Verlag GmbH, 2003), pp. 45–106.
[39]H. Wang, L. Wang, J. Sun, T. L. Guo, E. G. Chen, X. T. Zhou, Y. A. Zhang, and Q. Yan, "Role of surface microstructure and shape on light extraction efficiency enhancement of GaN micro-LEDs: A numerical simulation study," Displays 73, 102172 (2022).
[40]A. Tanaka, R. Chen, K. L. Jungjohann, and S. A. Dayeh, "Strong geometrical effects in submillimeter selective area growth and light extraction of GaN light emitting diodes on sapphire," Sci. Rep. 5, 17314 (2015).
[41]P. Vennéguès, B. Beaumont, V. Bousquet, M. Vaille, and P. Gibart, "Reduction mechanisms for defect densities in GaN using one- or two-step epitaxial lateral overgrowth methods," J. Appl. Phys. 87(9I), 4175–4181 (2000).
[42]S. Gradečak, P. Stadelmann, and V. Wagner, "Bending of dislocations in GaN during epitaxial lateral overgrowth," Appl. Phys. Lett. 85, 4648 (2004).
[43]W. Bergbauer, M. Strassburg, C. H. Kölper, N. Linder, C. Roder, J. Lähnemann, A. Trampert, S. Fündling, S. F. Li, H. H. Wehmann, and A. Waag, "Continuous-flux MOVPE growth of position-controlled N-face GaN nanorods and embedded InGaN quantum wells," Nanotechnology 21(30), 305201 (2010).
[44]M. Wehbe, M. Charles, K. Baril, B. Alloing, D. Pino Munoz, N. Labchir, J. Zuniga-Perez, C. Detlefs, C. Yildirim, and P. Gergaud, "Study of GaN coalescence by dark-field X-ray microscopy at the nanoscale," J. Appl. Crystallogr. 56(3), 643–649 (2023).
[45]Y. S. Cho, H. Hardtdegen, N. Kaluza, R. Steins, G. Heidelberger, and H. Lüth, "The growth mechanism of GaN with different H_2/N_2 carrier gas ratios," J. Cryst. Growth 307(1), 6–13 (2007).